ANL-HEP-159872

Physics potential of timing layers in future collider detectors

S.V. Chekanov[a], A.V. Kotwal[c], C.-H. Yeh[b], S.-S. Yu[b]

[a] *HEP Division, Argonne National Laboratory, 9700 S. Cass Avenue, Argonne, IL 60439, USA.*
[b] *Department of Physics and Center for High Energy and High Field Physics, National Central University, Chung-Li, Taoyuan City 32001, Taiwan*
[c] *Department of Physics, Duke University, USA*

Abstract

The physics potential of timing layers with a few tens of pico-second resolution in the calorimeters of future collider detectors is explored. These studies show how such layers can be used for particle identification and illustrate the potential for detecting new event signatures originating from physics beyond the standard model.

Keywords:

1. Introduction

Future particle colliders such as CLIC [1], the International Linear Collider (ILC) [2], the high-energy LHC (HE-LHC), and *pp* colliders of the European initiative, FCC-hh [3] and the Chinese initiative (CEPC [4] and SppC [5]) will motivate high-precision measurements of particles and jets at large transverse momenta. Timing information in these experiments can be used to improve particle and jet reconstruction and to suppress backgrounds. For example, high-precision timing will be beneficial for b-tagging for post-LHC experiments. At CLIC and FCC, high-precision time stamping of calorimeter energy deposits will be essential for background rejection (i.e. fake energy deposits) and pile-up mitigation. Precise timing information improves reconstruction of particle-flow objects by reducing overlap of out-of-time energy showers in highly-granular calorimeters.

Timing layers can be used for detection of long-lived particles and identification of standard model (SM) particles. Conceptual design reports for future experiments have not yet fully explored the benefits of the time-of-flight (TOF) measurements with calorimeters having tens-of-picosecond resolution.

In this paper we investigate the benefits of timing layers with resolution in the range 10 ps – 1 ns. The resolution of 1 ns is standard for existing and planned calorimeters [1, 2, 3, 5], and is used as a benchmark for comparisons with the more challenging 10 – 20 ps resolution devices. In addition, we investigate the capabilities of timing layers for

Email addresses: chekanov@anl.gov (S.V. Chekanov), ashutosh.kotwal@duke.edu (A.V. Kotwal), a9510130375@gmail.com (C.-H. Yeh), syu@cern.ch (S.-S. Yu)

identification of heavy stable particles which may be produced due to physics beyond the standard model (BSM). These studies can help shape the requirements for future calorimeters, which were already outlined in the CPAD report [6] that emphasized the need to develop fast calorimetric readouts.

2. Proposal

A generic design of calorimeters for future collider experiments is based on two main characteristics: (1) high-granularity electromagnetic (ECAL) and hadronic (HCAL) calorimeters with cell sizes ranging from 3×3 mm^2 to 5×5 cm^2. (2) timing with a nanosecond precision that improves background rejection, vertex association, and detection of new particles. According to the CPAD report [6], the development of "picosecond time resolution" for calorimeters is one of the critical needs. Presently, high-granularity calorimeters with > 1 million channels and with tens of picosecond resolution represent a significant challenge due to the large cost.

As part of the HL-LHC upgrade program, CMS and ATLAS experiments are designing high-precision timing detectors with resolution of about 30 ps [7, 8]. They are based on silicon sensors that add an extra "time dimension" to event reconstruction. In the case of the CMS High Granularity Calorimeter [9], six million channels of the endcap calorimeter require a dedicated front-end with $\simeq 20$ picosecond time binning.

As mentioned above, timing capabilities have not been fully explored for detectors beyond the HL-LHC upgrade, such as the ECAL and HCAL of the future detectors for the CLIC, CEPC, FCC and SppC experiments. It is considered an expensive option for the many millions of channels of these highly granular detectors, assuming that high-precision timing is implemented for all calorimeter cells. This opens an opportunity to investigate a cost-effective "timing layer", with time resolution better than 30 ps, to be installed in front of barrel and endcap calorimeters.

In this paper we will investigate the physics advantages of such timing layers in the post-LHC experiments. Typically, thin detectors in front of calorimeters are called "preshower", and were used in the ZEUS, CDF, ATLAS and CMS experiments. Their design goal is to count the number of charged particles in order to correct for upstream energy losses. The timing information of minimum-ionizing particles (MIP) has not been used for particle identifications or event timing. Unlike the standard preshower detectors, we propose to not only count MIP signals, but also measure high-precision timing and position of the MIPs. This timing detector will have a similar granularity as the proposed high-granularity ECALs, but will have sensor and readout technology that are best suited for time-stamping of MIP signals. Our proposal is to enclose the ECALs with two timing layers, one before the first EM layer, and the other after the last ECAL layer (but before the first HCAL layer). The two timing layers allow a robust calculation of time stamps by correlating the position and timing of the particles passing through the ECAL.

We explore this idea using a semi-analytical approach and using Monte Carlo simulations. A schematic representation of the positions of the timing layers for a generic detector geometry is shown in Fig. 1. In the following, the first timing layer (closest to the interaction point) will be called TL1, while the second timing layer after the ECAL will be called TL2.

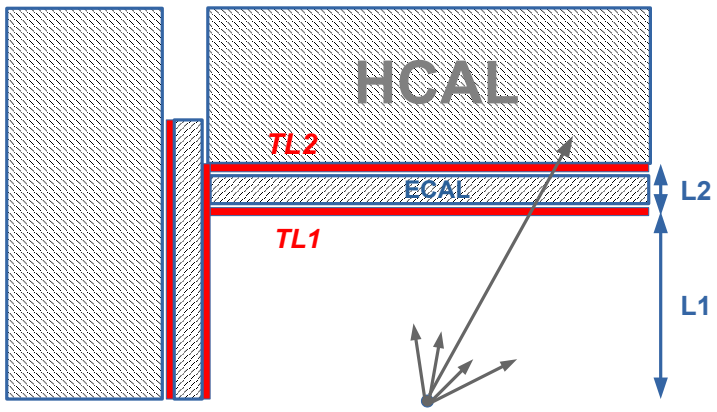

Figure 1: Example positions of thin timing layers for a generic detector. The timing detectors enclose the electromagnetic calorimeter, allowing a reliable calculation of the MIP signals with a timing resolution of the order of 10 ps.

There are several reasons why the second timing layer (TL2) can be useful:

- It can be used to measure the TOF between TL2 and TL1 for identification of stable massive particles without a known production vertex. This is especially important for BSM models predicting stable heavy particles decaying close to the surface of the ECAL, or in the situations when tracks cannot be used to establish the production vertex for neutral heavy particles. For proton colliders, the second layer can mitigate situations when the primary vertex position is smeared due to large pileup.

  For a typical ECAL based on silicon technology, the distance between TL2 and TL1 is 20 – 40 cm, depending on the calorimeter design. It is not immediately obvious that such a small distance can be used for physics measurements. A particle traveling at the speed of light can cross this distance within ~ 1 ns. As we will discuss later, this distance is sufficient to provide a large acceptance for heavy particle identification assuming 10 – 20 ps resolution detectors.

- It allows to correlate the hits with the first layer, and thus provide directionality of the hits. This feature can be useful to match the hits with the calorimeter cells and to deal with back-scatter hits which are typically arriving from the HCAL at a later time.

- It provides redundancy for the calculation of TOF using the distance from the production vertex determined using tracks.

The second layer of the timing detector can be justified if the recorded time difference between the first and the last ECAL layers of the electromagnetic showers is not significantly different from that expected from a particle traveling with speed of light. If the travel time is significantly affected by large fluctuations caused by electromagnetic showers, the second timing layer cannot be used effectively.

In order to verify this point, we used a full GEANT4 (version 10.3) [10] simulation of the SiFCC detector [11] that allows the use of the ECAL hit information. This detector design has an ECAL built from highly segmented silicon-tungsten cells with transverse size 2×2 cm^2. The ECAL has 30 layers of tungsten pads with silicon readout, corresponding to 35 X_0. The first 20 layers use tungsten of 3 mm thickness, while the last ten layers use tungsten layers of twice the thickness, and thus have half the sampling fraction. The distance between the centers of the first and last ECAL layers is about 24 cm.

To check that the time differences between the last and the first ECAL layer is close to the time required for a particle that travels with the speed of light, two samples of single pions ($\pi^{\pm}$) with momenta of 1 and 10 GeV respectively were created. The pseudorapidity (η) for all pions was fixed at $\eta = 0$ (central region). The particles were reconstructed in the ECAL, and the time difference $\Delta T = T_{\text{last}} - T_{\text{first}}$ of the hits between the last and first ECAL layers was calculated. Only the hits arriving first in time were considered since the electronics typically register[1] the fastest hits, while slower hits can be saved in pipeline buffers.

Figure 2 shows the time distribution of the earliest hits for 1 and 10 GeV pions. It can be seen that the peak positions of the distributions are smaller than 1 ns, as expected for the distance of 24 cm between the last and first ECAL layers. Therefore, the hits registered by TL1 and TL2 will be considered simultaneous for the standard 1 ns resolution readout. They will be fully correlated in time, and will be identified as a single crossing particle.

If the resolution of the timing layer is of the order of 10 – 20 ps, TOF can be used to identify particles which are heavier than pions. To check this, the arraval time of the earliest hits was calculated for (anti) deuterons (denoted as $d^{\pm}$) using the same simulation setup as before. Deuterons are 14 times heavier than pions, can be produced in the primary interactions, and their interaction with the detector material is well understood. If the difference between hit arraval times for $\pi^{\pm}$ and $d^{\pm}$ are larger than 20 ps, this would indicate a sensitivity of tens-of-picosecond detectors to particles with different masses.

Fig. 2 shows the time distribution of the earliest hits for $d^{\pm}$. The distributions are significantly different from the $\pi^{\pm}$ case. According to the simulation, the 1 GeV (anti)deuterons should be measured with the time delay of 0.7 – 1.4 ns between the last and first layers. The value of 0.7 ns was estimated from the peak of the Landau distribution used to fit the $d^{\pm}$ curve presented in Fig. 2(a), while 1.4 ns was obtained from the mean of this distribution. Even for the most conservative 0.7 ns value, this indicates that 1 GeV deuterons can be separated from pions that have 0.5 ns time difference. Such a separation can be observed using a tens-of-picosecond detector since the hits produced by the electromagnetic shower are sufficiently fast.

[1] The Monte Carlo studies in this paper do not include a simulation of calorimeter electronics.

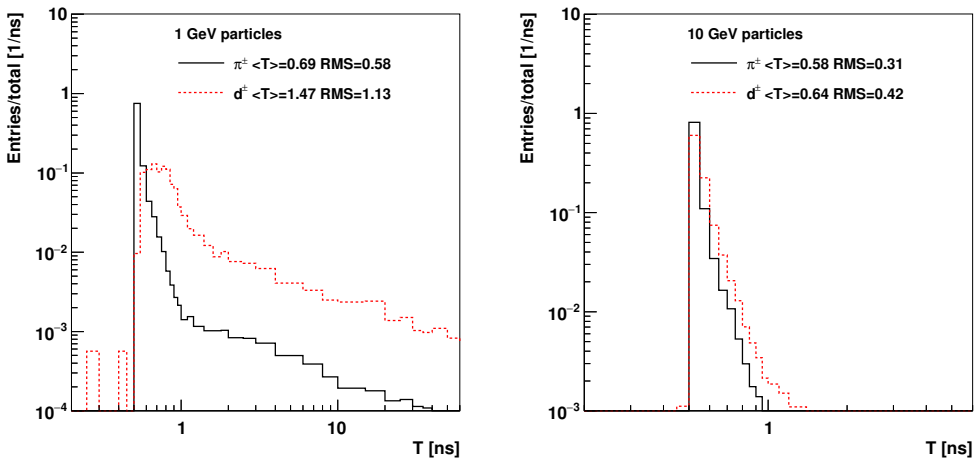

(a) (b)

Figure 2: Difference between hit times at the last and first layer of ECAL for single pions and deuterons with momentum of (a) 1 GeV and (b) 10 GeV. Only the earliest hits at each layer were considered in the calculation of the TOF.

For particle identification in realistic collider environments, 1 GeV range momentum range is rather low. For the 10 GeV particles shown in Fig. 2(b), no separation between $d^{\pm}$ and $\pi^{\pm}$ can be observed. This result is totally expected since the masses of pions and deuterons are small for effective separation of these particles at a momentum above 10 GeV.

In summary, we have illustrated that a typical difference between TL2 and TL1 (which is approximated by the difference between the last and first ECAL layer) is sufficient for particle identification using the TOF. As an example, a $d^{\pm}$ can be identified and separated from pions for momentum less than 1 GeV. However, particles heavier than deuterons should be identifiable for a momentum larger than 1 GeV. In the following, we will abstract from the GEANT4 simulations and calculate the kinematic regions where the identification of heavy stable particles using timing layers is possible.

3. Timing layers for single particles

Now we discuss the kinematic regions relevant for TOF measurements of SM and BSM particles. Instead of the full GEANT4 simulations, we will use a semi-analytic approach.

To estimate the separation power between different mass hypotheses, we calculate the mass and momentum for which one can achieve a separation significance higher than 3σ (or p-value$<$ 0.3%). If there are two particles with mass m and a reference (fixed) mass m_F, respectively, the 3σ separation can be achieved for this condition [12]:

$$\frac{L}{c\sigma_{\rm TOF}}\left|\sqrt{1+\frac{m^2}{p^2}}-\sqrt{1+\frac{m_F^2}{p^2}}\right|>3 \tag{1}$$

where p is the momentum of a particle with mass m, L is the length of the particle's trajectory, and σ_{TOF} is the resolution of the timing layer that measures the TOF.

Figure 3 shows the 3σ separation from the pion mass hypothesis ($m_F = m_\pi$) using the procedure discussed in [12]. The calculations are performed for several values of resolution of the timing layer, ranging from 10 ps to 1 ns, as a function of L and p. For a 20 ps detector and a typical travel distance $L \sim 1.5-2$ m from the production vertex to the ECAL, neutrons and protons can be separated from the pion hypothesis up to $p \approx 7$ GeV. The separation of kaons from pions can be performed up to 3 GeV. This momentum range should be sufficient for a reliable particle identification in a momentum range adequate for some physics studies focused on single-particle reconstruction (such as B-meson physics). This can also be used for jets that are dominated by particles in this momentum range. For a detector with 1 ns resolution, the separation can only be possible up to 300 – 500 MeV. This is smaller than the minimum particle momentum of ≈0.5 GeV considered for high-energy proton colliders. Therefore, a timing layer with 1 ns resolution cannot be used for particle identification in such experiments.

Having discussed the rather classical cases of discriminating neutrons, protons and kaons from the pion hypothesis, let us turn to the BSM searches for heavy particles. The largest SM backgrounds for light BSM particles are primary protons and neutrons. Other stable particles that can be produced by secondary interactions in the detector material or the beam pipe are deuterons and α particles. Although the α particle rate is low since they stop easily in detector material, it may still represent background for rare BSM particle searches. Therefore, we choose $m_F = m_\alpha \simeq 3.73$ GeV as reference[2] in Eq. 1, and evaluate the 3σ separation for a wide range of masses and momenta above 4 GeV. For many planned experiments the distance between the pp collision point and the first layer of the ECAL is $1.5-2.5$ m. Therefore we use $L = 2$ m and consider 0.2 m as the separation between the TL2 and TL1 timing layers.

Figure 4 shows the discrimination power for different choices of the timing layer resolution and the distance L (see Fig. 1). For $L = 2$ m, a stable heavy particle of mass 100 GeV can be discriminated for momentum up to 700 GeV assuming a 20-ps timing layer, but only up to 50 GeV using the standard 1 ns resolution.

[2]We clarify that the choice of α particles as the reference mass is arbitrary and is only motivated by our attempt to check the 3σ separation in the momentum range $p < 10$ GeV.

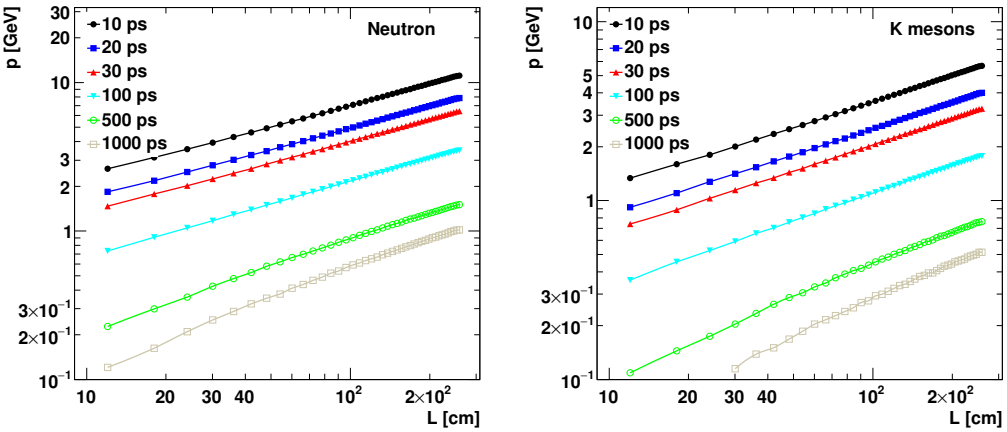

(a) Neutrons (b) K-mesons

Figure 3: The 3σ separation from the pion-mass hypothesis for (a) neutrons and (b) kaons as a function of the length of the particle's trajectory L and the momentum p. The lines show extrapolated results between the calculations indicated by the symbols.

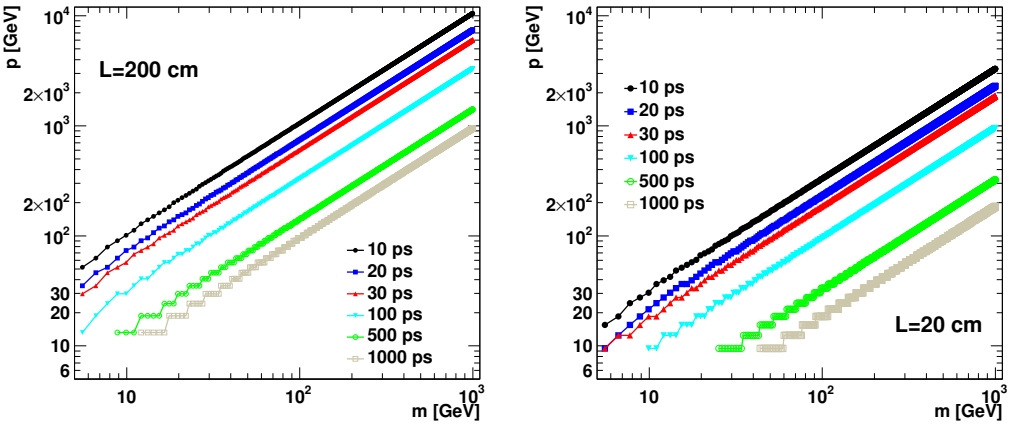

(a) for $L = 2$ m (b) for $L = 0.2$ m

Figure 4: The 3σ separation between heavy particles and α particles assuming timing layers with different resolutions for TOF, and using (a) $L = 2$ m and (b) $L = 0.2$ m. The first value of L is the typical distance from the interaction vertex to the first layer TL1, while the second value is the typical distance between the two timing layers enclosing an ECAL based on the silicon technology.

When TOF is measured between the layers TL1 and TL2, and assuming a spatial match of the hits, the knowledge of the interaction vertex is not required. This type of measurement can be beneficial for neutral particles in events with large pile-up (multiple pp collisions). The identification power when $L = 0.2$ m, i.e. the distance between TL2 and TL1, is shown in Fig. 4(b). For a stable particle with mass 100 GeV, the identification is possible up to about 200 GeV in momentum. The standard calorimeter with 1 ns resolution can only perform the identification up to 20 GeV.

4. Showcase for the Dark QCD model

The arguments discussed above can be illustrated using concrete BSM physics scenarios. We will consider the "dark" QCD model [13, 14], which predicts the existence of "emerging" jets that are created in the decays of new long-lived neutral particles (dark hadrons), produced in a parton-shower process by dark QCD. The process includes two mediators of mass M_X which decay promptly to a SM quark and a dark quark. The final-state signature consists of four jets with high transverse momenta, with two emerging jets originating from the dark quarks.

Searches for emerging jets have been performed in pp collisions [15] by the CMS Collaboration. Such jets contain many displaced vertices and multiple tracks with large impact parameters, arising from the decays of the dark pions produced in the dark parton shower. Assuming that the mass of the dark pion is 5 GeV, the signal acceptance using this approach does not exceed 40% at large masses of the mediators (see Fig. 4 of [15]). The decay length of the dark pion defines the distance from the pp interaction vertex to the point where the jet emerges.

Alternatively, emerging jets can be reconstructed using calorimeters with high-resolution timing. This method is expected to have advantages over the track-based method for the measurement of dark pions with a large decay length, i.e. in the situations where the tracker has a low efficiency and resolution since only a few outer layers can be used for track reconstruction. It was also pointed out [14] that the emerging jets may have a significant fraction of neutral particles and the reconstruction using charged tracks can have a low acceptance.

To estimate the performance of the timing layers in reconstructing emerging jets, we use the same Monte Carlo generator settings as for Ref. [15]. The pp collision event samples were generated with the "hidden valley" model framework as implemented in PYTHIA 8.2 [16] assuming a centre-of-mass energy of 13 TeV and a dark pion mass of 5 GeV. The samples were created for different values of the decay distance $c\tau$ of the dark pions. The mass M_X of the mediator was also varied.

To calculate the detector acceptance, the semi-analytical formalism based on Eq. 1 is used. In this relation $L = c\tau$ is the distance traveled by the dark pion with mass m before it decays to the emerging jet. We assume that such emerging jets travel to the surface of the timing layer with speed of light for all values of m. This is expected since the emerging jets consist of light stable SM particles (mostly photons and pions).

For the timing layers, the signature of emerging jets is a time delay compared to the other SM jets. The production vertex cannot be observed by the timing layers if such jets emerge before TL1. After events are generated, the weighted averages of the decay distances of all particles that originate from the dark pions, using the particle

momentum as the weight, were calculated. This decay distance is used to approximate the decay length, without applying a jet reconstruction algorithm. The calculation for the 3σ separation assumes $m_F = m_\alpha \simeq 3.73$ GeV although this choice can be arbitrary. This value of m_F is used to give a conservative[3] estimate of the arrival time of the emerging SM jets.

The acceptance of the emerging jets was calculated as the fraction of events that pass the Eq. 1 condition with the parameters discussed earlier. Figure 5 shows the acceptance as a function of the mediator mass M_X and the decay distance of the dark pions. This acceptance can be compared to the acceptance based on tracks [15]. The acceptance based on the TOF is significantly larger for low M_X and large $L = c\tau$ of the dark pions. The acceptance is larger for the timing layers with a resolution better than 100 ps, as compared to the standard 1 ns resolution.

We are interested in the acceptance for dark pions as a function of their mass and lifetime assuming a fixed mass M_X of the mediator. We consider the HE-LHC environment with pp collisions at a centre-of-mass energy of 27 TeV. The Monte Carlo generator settings for the signal model were similar to those discussed in [15, 17]. The mediator mass was set to 10 TeV, while the mass of the dark pion was varied in the range between 5 GeV and 1 TeV. The dark pion decay length, $c\tau$, was varied between 1 mm and 1000 mm, independent of its mass. Other parameters were also appropriately modified to allow sufficient phase space for the dark meson production. The mass of the dark pion is assumed to be one half the mass of the dark quark. The mass of the dark ρ is four times the dark pion mass. The width of the mediator particle is assumed to be small compared to the detector mass resolution.

As before, the acceptance for the emerging jets based on timing was calculated as the fraction of events that pass the Eq. 1 condition. Figure 6 shows the efficiency as a function of $c\tau$ and the dark pion mass. It can be seen that a detector with the standard 1 ns resolution does not have acceptance for the dark meson measurements. The acceptance is significantly larger when the timing layers have a resolution better than 100 ps. The acceptance is low for small $c\tau$ or small masses, which is the expected feature of the timing measurement. The timing layers with 20 ps resolution have 100% acceptance for large values of $c\tau$ and dark-meson masses. The acceptance as a function of the particle velocity when using 20 ps and 1 ns resolution is shown in Appendix A.

Note that these results are relatively general since they are formulated in terms of masses and decay lengths, i.e. independent of the position of the timing layers and other details relevant to the detector geometry.

5. Summary

This paper discusses the benefits of timing layers positioned in front of the hadronic calorimeters. Using the full GEANT4 simulation and a semi-analytic approach, the figures of merit for the identification of single particles using timing layers with resolutions of 10 ps – 1 ns were calculated. It was illustrated how such layers can be used for single-particle identification and discrimination of heavy long-lived particles in the context of

[3] One can argue that the SM jets mainly consist of light-flavour hadrons and photons, therefore, m_F should be significantly lower.

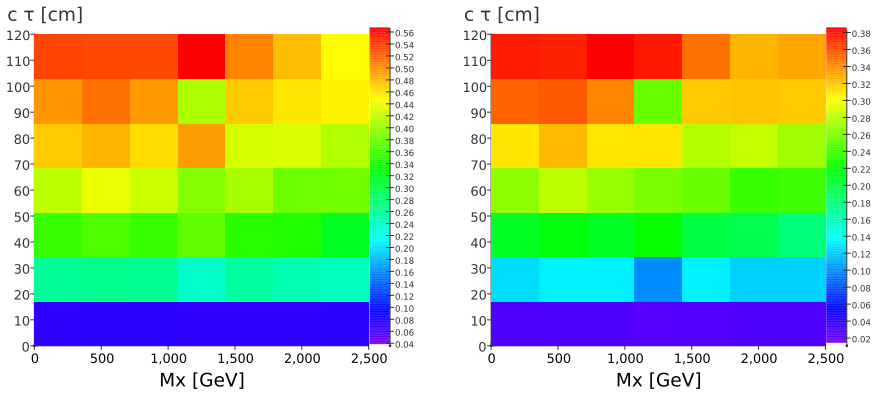

(a) 10 ps

(b) 20 ps

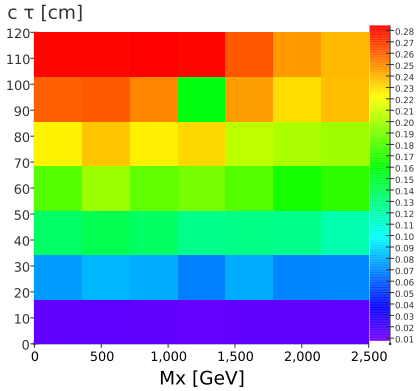

(c) 30 ps

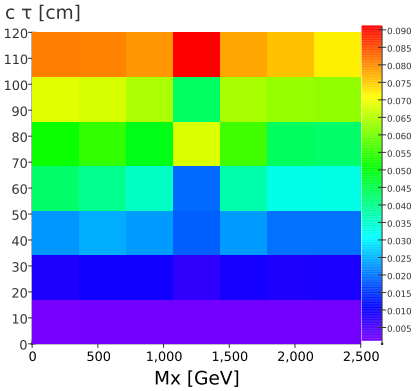

(d) 100 ps

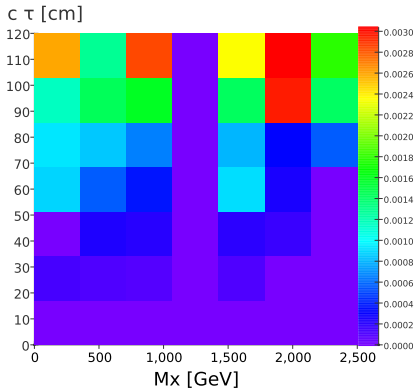

(e) 500 ps

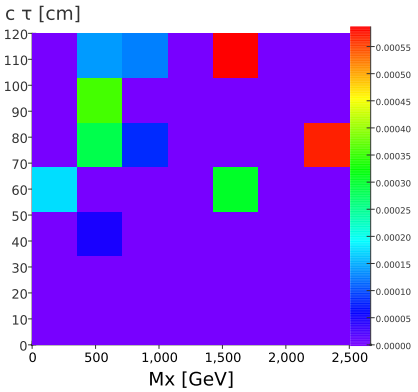

(f) 1000 ps

Figure 5: The acceptance for emerging jets using timing layers with different timing resolutions as a function of the mediator mass M_X and the $c\tau$ of the dark pions with mass of 5 GeV. The PYTHIA8 simulations were performed for pp collisions at $\sqrt{s} = 13$ TeV. The maximum values for the color mapping vary from 0.56 (a) to 0.0006 (f).

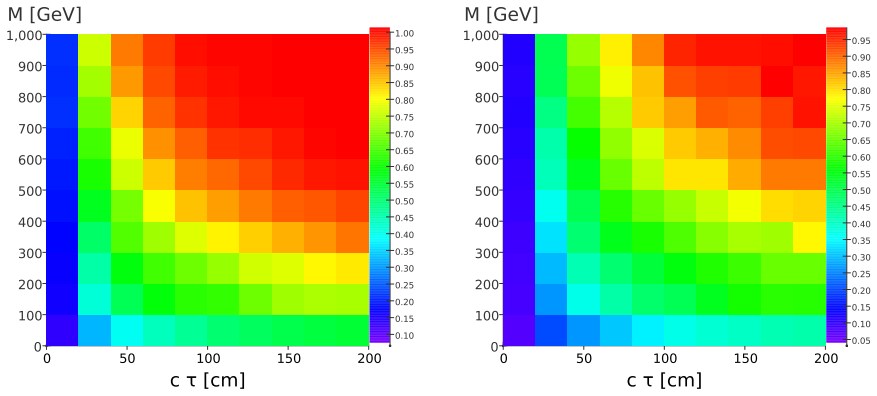

(a) 10 ps

(b) 20 ps

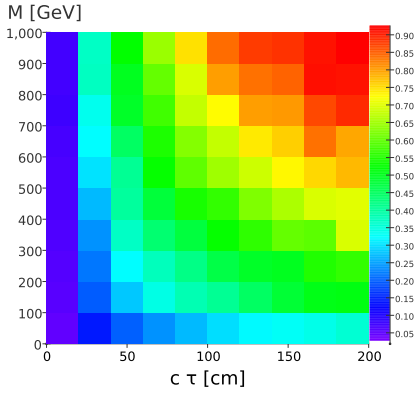

(c) 30 ps

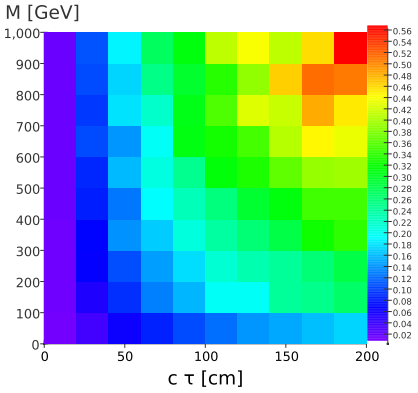

(d) 100 ps

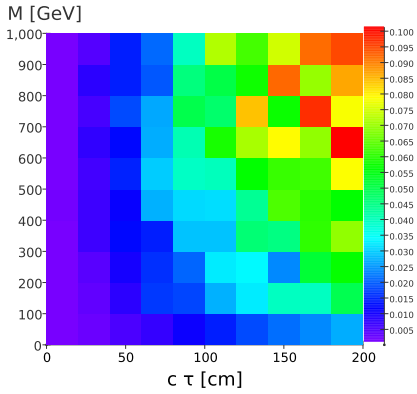

(e) 500 ps

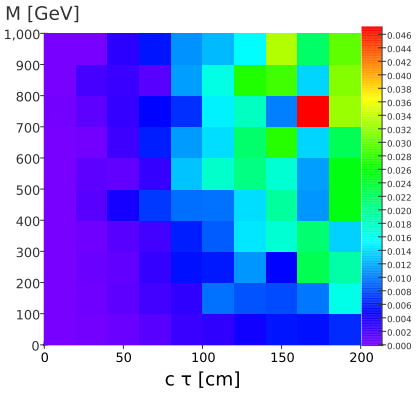

(f) 1000 ps

Figure 6: The acceptance for emerging jets using timing layers with different timing resolutions as a function of the dark pion mass and $c\tau$. The mediator mass was fixed at $M_X = 10$ TeV. The PYTHIA8 simulations were performed for pp collisions at $\sqrt{s} = 27$ TeV. The maximum values for the color mapping vary from 1.0 (a) to 0.046 (f).

the dark QCD model. It was shown that the timing layers lead to a significant benefit for reconstruction of heavy long-lived particles in the range of $c\tau$ and momentum where track-based measurements have low acceptance.

Acknowledgments

The Monte Carlo events were generated using resources provided by the Open Science Grid, which is supported by the National Science Foundation award 1148698, and the U.S. Department of Energy's Office of Science. We gratefully acknowledge the computing resources provided on a high-performance computing cluster operated by the Laboratory Computing Resource Center at Argonne National Laboratory. The submitted manuscript has been created by UChicago Argonne, LLC, Operator of Argonne National Laboratory ("Argonne"). Argonne, a U.S. Department of Energy Office of Science laboratory, is operated under Contract No. DE-AC02-06CH11357. The U.S. Government retains for itself, and others acting on its behalf, a paid-up nonexclusive, irrevocable worldwide license in said article to reproduce, prepare derivative works, distribute copies to the public, and perform publicly and display publicly, by or on behalf of the Government. Argonne National Laboratory's work was funded by the U.S. Department of Energy, Office of High Energy Physics under contract DE-AC02-06CH11357.

References

[1] L. Linssen, A. Miyamoto, M. Stanitzki, H. Weerts, Physics and Detectors at CLIC: CLIC Conceptual Design Report, CERN Yellow Reports: Monographs, CERN, Geneva, 2012, comments: 257 p, published as CERN Yellow Report CERN-2012-003. doi:10.5170/CERN-2012-003.
URL http://cds.cern.ch/record/1425915

[2] T. Behnke, J. E. Brau, B. Foster, J. Fuster, M. Harrison, J. M. Paterson, M. Peskin, M. Stanitzki, N. Walker, H. Yamamoto, The International Linear Collider Technical Design Report - Volume 1: Executive SummaryarXiv:1306.6327.

[3] M. Benedikt, The Global Future Circular Colliders EffortCERN-ACC-SLIDES-2016-0016. Presented at P5 Workshop on the Future of High Energy Physics, BNL, USA, Dec. 15-18, 2013.
URL http://cds.cern.ch/record/2206376

[4] CEPC Study Group, CEPC Conceptual Design Report: Volume 2 - Physics & DetectorIHEP-CEPC-DR-2018-02, IHEP-EP-2018-01, IHEP-TH-2018-01. arXiv:1811.10545.

[5] J. Tang, et al., Concept for a Future Super Proton-Proton Collider (2015). arXiv:1507.03224.

[6] Z. Ahmed, et al., New Technologies for Discovery, in: CPAD Instrumentation Frontier Workshop 2018: New Technologies for Discovery IV (CPAD 2018) Providence, RI, United States, December 9-11, 2018, 2019. arXiv:1908.00194.
URL https://lss.fnal.gov/archive/2019/conf/fermilab-conf-19-487-di-nd-ppd-scd.pdf

[7] ATLAS Collaboration, Technical Proposal: A High-Granularity Timing Detector for the ATLAS Phase-II Upgrade, Tech. Rep. CERN-LHCC-2018-023. LHCC-P-012, CERN, Geneva (Jun 2018).
URL http://cds.cern.ch/record/2623663

[8] CMS Collaboration, A MIP Timing Detector for the CMS Phase-2 Upgrade, Tech. Rep. CERN-LHCC-2019-003. CMS-TDR-020, CERN, Geneva (Mar 2019).
URL https://cds.cern.ch/record/2667167

[9] CMS Collaboration, The Phase-2 Upgrade of the CMS Endcap Calorimeter, Tech. Rep. CERN-LHCC-2017-023. CMS-TDR-019, CERN, Geneva, technical Design Report of the endcap calorimeter for the Phase-2 upgrade of the CMS experiment, in view of the HL-LHC run. (Nov 2017).
URL https://cds.cern.ch/record/2293646

[10] J. Allison, et al., Recent developments in Geant4, Nuclear Instruments and Methods in Physics Research A 835 (2016) 186.

[11] S. V. Chekanov, M. Beydler, A. V. Kotwal, L. Gray, S. Sen, N. V. Tran, S. S. Yu, J. Zuzelski, Initial performance studies of a general-purpose detector for multi-TeV physics at a 100 TeV pp collider, JINST 12 (06) (2017) P06009. arXiv:1612.07291, doi:10.1088/1748-0221/12/06/P06009.

[12] O. Cerri, S. Xie, C. Pena, M. Spiropulu, Identification of Long-lived Charged Particles using Time-Of-Flight Systems at the Upgraded LHC detectors, JHEP 04 (2019) 037. arXiv:1807.05453, doi:10.1007/JHEP04(2019)037.

[13] Y. Bai, P. Schwaller, Scale of dark QCD, Phys. Rev. D89 (6) (2014) 063522. arXiv:1306.4676, doi:10.1103/PhysRevD.89.063522.

[14] P. Schwaller, D. Stolarski, A. Weiler, Emerging Jets, JHEP 05 (2015) 059. arXiv:1502.05409, doi:10.1007/JHEP05(2015)059.

[15] CMS Collaboration, A. M. Sirunyan, et al., Search for new particles decaying to a jet and an emerging jet, JHEP 02 (2019) 179. arXiv:1810.10069, doi:10.1007/JHEP02(2019)179.

[16] T. Sjostrand, S. Mrenna, P. Z. Skands, A Brief Introduction to PYTHIA 8.1, Comput. Phys. Commun. 178 (2008) 852–867. arXiv:0710.3820.

[17] K. Pedro, P. Schwaller, Private communication. We thank Dr. P.Kevin and P.Schwaller for help with the setup of Monte Carlo generation parameters.

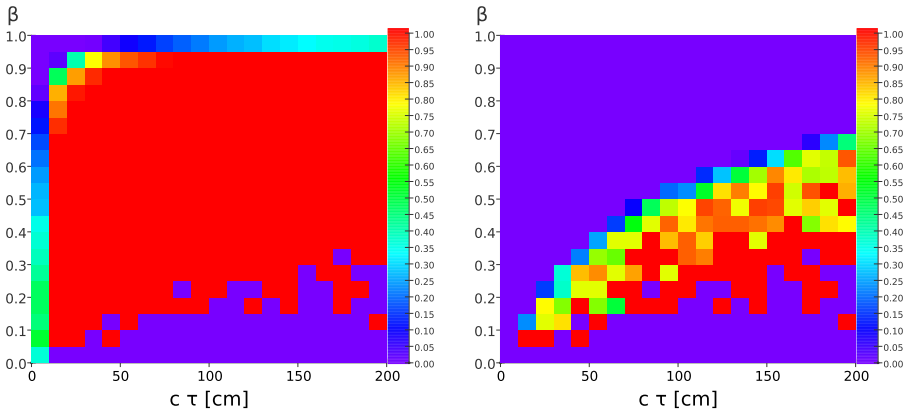

(a) 20 ps (b) 1000 ps

Figure A.7: Acceptance for the reconstruction of emerging jets using the timing layers with different timing resolutions. The histogram shows the acceptance as a function of $c\tau$ and the particle velocity β.

Appendix A. Acceptance vs β

Figure A.7 shows the reconstruction acceptance as a function of $c\tau$ and the particle velocity $\beta = |p|/E$, for the two extreme cases of the timing layers. The calculations were performed using the Monte Carlo simulations for emerging jets (see the text).